Thermal Stability of Ultra-Thin Co Recording Media

Heng Gong, Wei Yang and David N. Lambeth
Maithri Rao* and David E. Laughlin*
Department of Electrical and Computer Engineering, Department of Materials Science and Engineering*
Data Storage Systems Center, Carnegie Mellon University, Pittsburgh, PA 15213

Abstract — **Ultra-thin Co/Cr films were fabricated by RF diode sputtering. The highly exchange coupled Co grains were successfully isolated by post deposition processing. The microstructure was studied with TEM and a very small physical grain size was observed. The measurement of ΔM curves showed that the grain to grain interaction changed from positive to negative. Time dependent magnetic measurements showed significant thermal decay effects. It was also found that the use of CrMn underlayers instead of pure Cr further isolated the Co grains.**

Index Terms — **Thermal stability, magnetic viscosity, superparamagnetism, magnetic recording media.**

I. Introduction

To maintain sufficient signal to noise ratio for future high density longitudinal recording, a very thin film structure with very small grains is desired. However, under this paradigm of medium evolution, the media will eventually become thermally unstable at ultra-high recording density due to the onset of superparamagnetism. The limitation on recording density imposed by thermal instability has been systematically simulated by micromagnetic modeling [1]. In this study, as a path to verification of these simulation results, very thin and small, thermally unstable pure Co film particles were prepared. Post deposition processing was employed to isolate the strongly exchange coupled Co grains so that the films would resemble the characteristics of ultra-high density recording media. The conventional, as well as the time dependent magnetic properties along with the thin film microstructures have been investigated. In an attempt to help test the validity of the micromagnetic simulation, the experimental results presented here are being used to test the modeling [2].

II. Experimental Procedure

Thin films were deposited by RF diode sputtering in a Leybold-Haereus Z-400 sputtering system. The base vacuum pressure was below 5×10^{-7} Torr. The RF sputtering power and Ar gas pressure were set to 2.25W/cm^2 and 10 mTorr, respectively. Corning 7059 glass was used as substrates for all samples. The substrates were pre-heated to about 260°C before deposition so that the Cr underlayer would develop a (002) texture and then induce the desired $(11\bar{2}0)$ textured Co film on top of it. Films with the Co layer thickness varying from 2.5 nm to 10 nm were deposited on underlayers of 30 nm thickness. In order to provide a clear comparison, four samples all with the same thickness of the Co layer are discussed here. The Co films of these four samples are all 5 nm thick. Samples A, B and C used a Cr underlayer and sample D used a CrMn alloy underlayer with 24at% Mn in order to further isolate the Co grains [3]. Sample A has a 15 nm thick Cr overcoat deposited immediately after the deposition of the Co film without breaking the vacuum. In order to avoid oxidization, samples A and B were cooled under vacuum before exposure to ambient air, while samples C and D were slightly oxidized by exposure to ambient air at elevated temperature shortly after deposition. The samples and processing methods are summarized in Table I.

TABLE I
STRUCTURE AND PROCESSING CONDITIONS OF SAMPLES

Sample	Film Structure	Oxidized
A	15 nm Cr/5 nm Co/30 nm Cr	No
B	5 nm Co/30 nm Cr	No
C	5 nm Co/30 nm Cr	Yes
D	5 nm Co/30 nm CrMn	Yes

III. Results and Discussion

Conventional hysteresis loops were measured using an alternating gradient magnetometer (AGM). The results are listed in Table II.

TABLE II
MAGNETIC PARAMETERS OF SAMPLES A, B, C AND D

Sample	H_c (Oe)	S	S^*	$M_s t$ (memu/cm^2)
A	510	0.91	0.92	0.55
B	705	0.92	0.85	0.60
C	1150	0.79	0.62	0.42
D	1300	0.68	0.61	0.35

The results show that both sample A and sample B have lower coercivities compared to samples C and D. The remanence squareness S and coercivity squareness S^* of A and B are also higher than those of C and D. These results indicate that samples A and B are strongly exchange coupled. Compared with A and B, the slightly oxidized samples C and D have much higher coercivities and lower S and S^* values. Assuming that the fundamental magnetocrystalline anisotropy has not increased, the improved coercivity cannot be accounted for by the simple decrease in the magnetic moment.

The intergranular interactions in the Co films were characterized by measuring the remnant magnetization ΔM

Manuscript received October 17, 1997.
Heng Gong, 412-268-2465, fax 412-268-6978, hgong@andrew.cmu.edu.
This work was supported in part by a grant from NSIC and by the DSSC at CMU under a grant from NSF, #ECD-8907068.

0018-9464/98$10.00 © 1998 IEEE

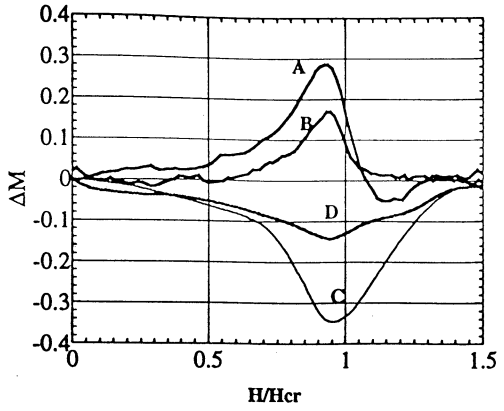

Fig. 1. ΔM curves of samples A, B, C and D.

curves. The $\Delta M(H)$ measurement technique for determining grain to grain interactions was introduced by Kelly *et al.* [4]:

$$\Delta M(H) = I_d(H) - [1 - 2\, I_r(H)] \qquad (1)$$

where $I_r(H)$ is the normalized isothermal remanence (ISR) curve, obtained through progressive magnetization of an initially demagnetized sample, and $I_d(H)$ is the normalized dc demagnetization remanence (DCR) curve, obtained through progressive demagnetization from a previously saturated state.

The ΔM curves for samples A, B, C and D are shown in Fig.1. Both samples A and B exhibit positive curve peaks while C and D exhibit negative peaks. This means that the intergranular interactions in samples A and B are dominated by exchange coupling, while in samples C and D are dominated by magnetostatic interaction. Since C and D are oxidized, the formation of an oxide shell on the Co grains may provide isolation. The differences in H_c, S and S^* values between samples A, B and C, D agree with the ΔM results. Compared to sample B, A has a 15 nm thick Cr overcoat deposited immediately after the deposition of the Co layer. Sample A's lower H_c, higher S^* value, and higher ΔM peak than those of sample B demonstrate a stronger intergranular exchange coupling than in sample B. The diffusion of Cr into the Co grain boundaries may enhance the exchange coupling. Alternatively, since there is no Cr overcoat, there may have been slight oxidization at Co grain boundaries in sample B. Contrary to the role of the Cr overcoat, it was also found that by using a 15 nm Ag overcoat, both the coercivity and remanent coercivity, Hcr, greatly increased and the ΔM curve showed a negative peak. The diffusion of Ag, which is insoluble in Co, into the grain boundaries may help isolate the grains. The magnetic properties of samples with the Ag overcoat were found to be very similar to the properties of the oxidized samples and will be discussed elsewhere. The difference between samples C and D is that D has a CrMn underlayer instead of pure Cr. Sample D exhibits both a higher coercivity and a smaller negative ΔM peak. The diffusion of Mn into the grain boundaries of the Co grains, as opposed to a voided grain boundary structure [5], may give rise to a better or a different intergranular interaction. Since Mn is insoluble in hcp Co, but is soluble in fcc Co, it may tend to remain at the grain boundaries. Or, since small amounts of Mn significantly increase the Neel temperature of Cr, the combined diffusion of Cr and Mn to the Co grain boundaries may result in antiferromagnetic coupling.

The microstructure of the samples have been studied with TEM. It is observed that the grain size of Co particles decreases with decreasing thickness of the Co layer. For the 5 nm thick samples, the grain size is around 10 nm. Fig. 2(a) shows a selected area diffraction pattern of sample D. The presence of very weak cobalt oxide rings indicate slight oxidization of the Co film. Fig. 2(b) shows the bright-field micrograph of sample D. The average grain size is also estimated to be around 10 nm. Since Co oxide is antiferromagnetic with a Neel point below room temperature, the magnetic properties of the films are anticipated to be dominated by the pure Co cores of the grains.

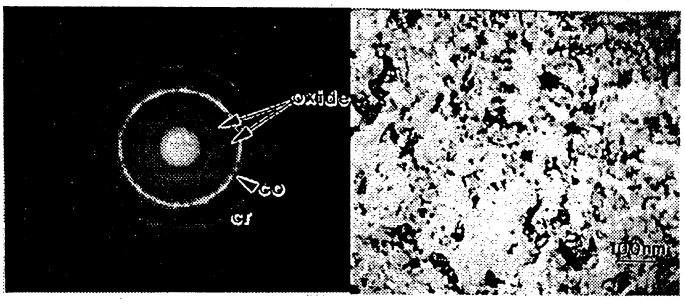

(a) Selected area diffraction pattern (b) Bright field micrograph

Fig. 2. TEM photographs of sample D.

In order to study thermal effects, the time dependent remanent coercivity was measured. Since the switching process is thermally assisted the measured coercivity is not an intrinsic property of the film, but depends upon the time spent at the applied field. The experimental procedure is to first saturate the sample, then at time zero to apply a step function reverse field. When the magnetization reaches zero, for a particular field magnitude, the time is recorded. By repeating this procedure at many field values a plot of the coercivity, H_c versus time is obtained.

The thermal activation volume V_{act} can then be determined from:

$$V_{act} = \frac{kT}{M_s H_f} \qquad (2)$$

where H_f is the fluctuation field [6]. The fluctuation field H_f is determined from the measurement of H_c vs ln(t) from:

$$t = t_0 \exp\left(-\frac{H_c - H_0}{H_f}\right) \qquad (3)$$

where H_0 is a reference field [7]. From the linear slope of H_c vs. ln(t), H_f and V_{act} can be obtained.

The time dependent coercivity curves of the four samples are shown in Fig. 3 where the coercivities were normalized by

their respective values obtained at 0.1 second. As anticipated, all four samples exhibit thermal decay in our measurement time frame. The decreasing coercivities of samples C and D are much more pronounced than those of samples A and B. This implies that the exchange coupled samples A and B have larger effective activation volumes. The slope of the curve for sample D is greater than that of sample C. Since these samples are prepared in the same manner, this better isolation or smaller grain size must be due to the underlayer composition difference. The calculated activation volumes, V_{act}, are listed in Table III.

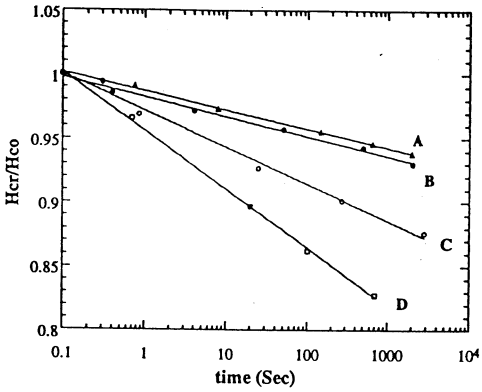

Fig.3 Time dependence of coercivity for A, B, C and D.

Table III
ACTIVATION VOLUMES FOR SAMPLES A~D

Sample	V_{act} (10^{-18} cm^3)
A	8.1
B	7.9
C	2.0
D	0.8

Since the same deposition conditions were employed and the magnetic grains tend to replicate the underlayer microstructure, the physical grain sizes of the four samples are similar to each other. The significant difference in the activation volume between A, B and C, D is due to the varying degree of intergranular exchange coupling.

The magnetic viscosity $S(H)$ is defined as:

$$M_r(H, t) = M_r(H, t_0) - S(H) \bullet M_S \bullet \ln(t/t_0) \qquad (4)$$

where H is the applied reverse field intensity and $M_r(H, t)$ is the observed remanent magnetization at time t after applying the reverse field. M_S is the saturation magnetization of the sample. Larger $S(H)$ values represent a faster decay of the magnetization.

As the reverse field approaches the remanent coercivity, the magnetic viscosity plots (Fig.4) show a dramatic increase in curvature for the exchange coupled samples A and B, while the well-isolated samples C and D yield rather flat curves. This indicates that the magnetization of the highly exchange coupled films will remain stable until the reverse field approaches the remanent coercivity while the magnetization of the isolated grains is thermally unstable even in fields much smaller than the coercivity.

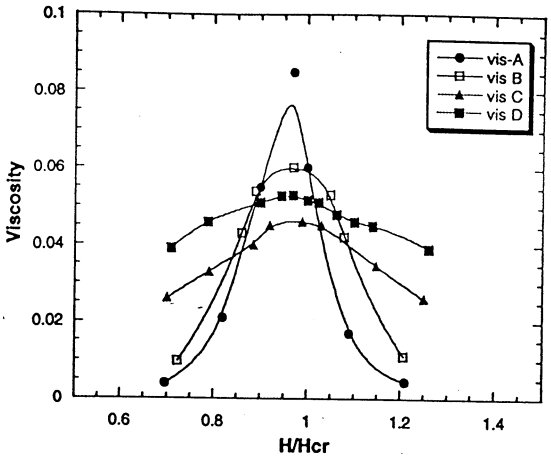

Fig. 4 Magnetic viscosity curves of samples A, B, C, and D.

IV. CONCLUSIONS

In this study, very small, thermally unstable Co film particles were prepared. Post-deposition exposure to atmosphere and CrMn underlayers were employed to isolate the strongly exchange coupled Co grains. After isolation, the coercivity values were greatly increased and ΔM peaks changed from positive to negative. The measurement of the time dependence of the coercivity, and the rapid coercivity decay, showed that the isolation technique was very effective in decoupling the grains. Magnetic viscosity curves showed a significant difference between the exchange coupled films and the decoupled films. From these measurements, it was found that the exchange coupled films only show magnetization decay in the vicinity of their coercivity. The isolated samples show significant thermal decay at a much wider range of reverse fields. In future high density longitudinal recording, well-isolated medium with small grain size is required in order to have low noise. However, our results indicate that this kind of media may suffer significant thermal decay in the presence of a demagnetization field. In the future, we hope to make actual recording disks using these preparation techniques and to investigate the time dependence of recorded data.

REFERENCES

[1] P. Lu and S. H. Charap, IEEE Trans. Magn. **30**, 4230(1994).
[2] H. Fang and J.-G. Zhu, to be published.
[3] L.-L Lee, D. E. Laughlin and D. N. Lambeth, the 1998 Joint MMM-Intermag Conference, CC-02.
[4] P. E. Kelly, K. O'Grady, P. I. Mayo, and R. W. Chantrell, IEEE Trans. Magn. **25**, 3881(1989).
[5] T. Yogi *et al*, IEEE Trans. Magn. **26**, 1579(1990).
[6] E. P. Wohlfarth, J. Phys. **F14**, 1155(1984).
[7] R. W. Chantrell, G. N. Coverdale, and K. O'Grady, J. Phys. **D21**, 1469(1988).